2005 WJTA American Waterjet Conference
August 21-23, 2005 • Houston, Texas

Paper 3A-3

ESTIMATION OF ABRASIVE MASS FLOW RATE BY MEASURING FEED LINE VACUUM DURING JET ON-OFF CYCLING

Ian Conner
The Boeing Company
Seattle, Washington

M. Ramulu
University of Washington
Seattle, Washington, USA

ABSTRACT

The abrasive waterjet cutting head is designed to draw air through the abrasive feed tube at a velocity adequate to maintain steady abrasive flow without saltation or slug formation. The air flow restrictions introduced by the abrasive feed tube and the inlet port lead to a partial vacuum condition within the mixing chamber, and a decreasing vacuum gradient along the tube length to its distal end, which is normally open to atmosphere. The strength of the chamber vacuum thus depends directly on the air entrainment rate of the water jet, as well as the amount of restriction present throughout the abrasive inlet passage. The abrasive flow must be precisely metered to avoid either overwhelming the jet and clogging the inlet, or starving the jet and reducing cutting power which affects the cut quality. This is usually accomplished by gravity-feeding the abrasive through a calibrated aperture that yields a predetermined mass flow rate for a particular abrasive mesh size. A variety of methods have been employed experimentally, but have found little practical application in industry. This paper explore various aspects of vacuum creation in an AWJ nozzle, particularly the role of the abrasive particles themselves in increasing the effective air flow resistance. The intent is to present an analytical framework for estimating abrasive mass flow rates based on continuous measurements of the vacuum level within the abrasive feed tube.

Organized and Sponsored by the Waterjet Technology association

1. INTRODUCTION

In a typical abrasive waterjet cutting head (Figure 1), the air inflow produced by passage of the high-velocity jet through the interior space is used to convey dry abrasive material into the mixing chamber. The strength of the air flow produced depends on several process conditions, most significantly the jet pressure, the orifice and mixing tube diameters, and the dimensions of the mixing chamber and abrasive inlet port. The cutting head is designed to draw air through the abrasive feed tube at a velocity adequate to maintain steady abrasive flow without saltation or slug formation. The air flow restrictions introduced by the abrasive feed tube and the inlet port lead to a partial vacuum condition within the mixing chamber, and a decreasing vacuum gradient along the tube length to its distal end, which is normally open to atmosphere. The strength of the chamber vacuum thus depends directly on the air entrainment rate of the water jet, as well as the amount of restriction present throughout the abrasive inlet passage.

The abrasive flow must be precisely metered to avoid either overwhelming the jet and clogging the inlet, or starving the jet and reducing cutting power. This is usually accomplished by gravity-feeding the abrasive through a calibrated aperture that yields a predetermined mass flow rate for a particular abrasive mesh size. Actual measurement and monitoring of the abrasive mass flow rate during jet operation is difficult, and is not performed on most automated AWJ cutting systems. A variety of methods have been employed experimentally, but have found little practical application in industry. The goal of this study is to explore various aspects of vacuum creation in an AWJ nozzle, particularly the role of the abrasive particles themselves in increasing the effective air flow resistance. The intent is to arrive at a framework for estimating abrasive mass flow rates based on continuous measurements of the vacuum level within the abrasive feed tube.

A central question to be addressed is whether the AWJ nozzle can be modeled as a generic vacuum source, tending to produce air flow in the feed tube at a rate which is not strongly dependent on abrasive/water mixing effects within the mixing chamber. If so the problem is simplified greatly, since the vacuum rise associated with the start of abrasive flow can then be attributed entirely to the restrictive effect of the abrasive particles moving through the feed tube. That is, the AWJ nozzle itself can be treated as a simple vacuum reservoir that seeks to draw air in at a fixed volumetric rate, and the vacuum difference between water-only operation and a fully-mixed abrasive jet will have a direct relationship to the abrasive mass flow rate.

Figure 2 shows the trajectory of a continuous vacuum signal as the jet and abrasive are cycled on and off in the usual sequence. When the jet turns on initially, only air is flowing through the abrasive feed tube, and the p_{v1} vacuum level depends only on the rate of this air flow and the fixed restrictions within the feed tube and mixing chamber inlet. When the abrasive flow begins, the vacuum rises asymptotically to the p_{v2} level, where it remains as long as the water and abrasive flows remain constant. When the abrasive flow stops, the vacuum drops abruptly back to the p_{v1} level as the feed tube is cleared of remaining abrasive material. The goal here is to relate the abrasive mass flow rate during steady-state AWJ operation to the difference between p_{v2} and p_{v1}.

Of course many factors besides the abrasive mass flow rate will influence the vacuum level produced under any nominal set of operating conditions. Orifice and mixing tube wear, particularly, lead to significant variations in air entrainment and vacuum creation over time. Alignment of the orifice and mixing tube are also critical for proper jet function [1]. Past efforts have been directed toward using vacuum measurement as a general indicator of the cutting nozzle condition [2]; however, the variety of independent contributing factors makes it difficult to isolate any single source of deviation in the measurements obtained. For the purposes of this paper, variables related to consumable part wear are not considered; all orifices and mixing tubes used for test measurements are in new condition and are assumed to retain their ideal, nominal dimensions throughout the test runs.

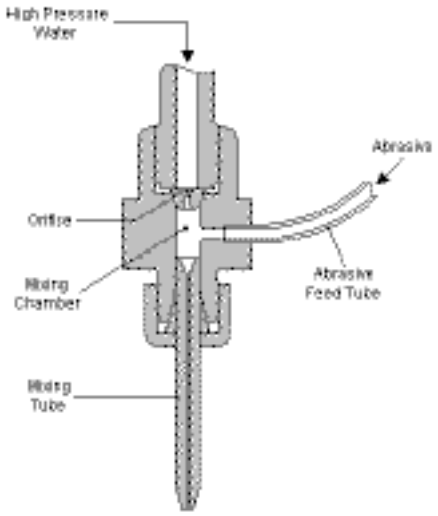

Figure 1: AWJ cutting head components

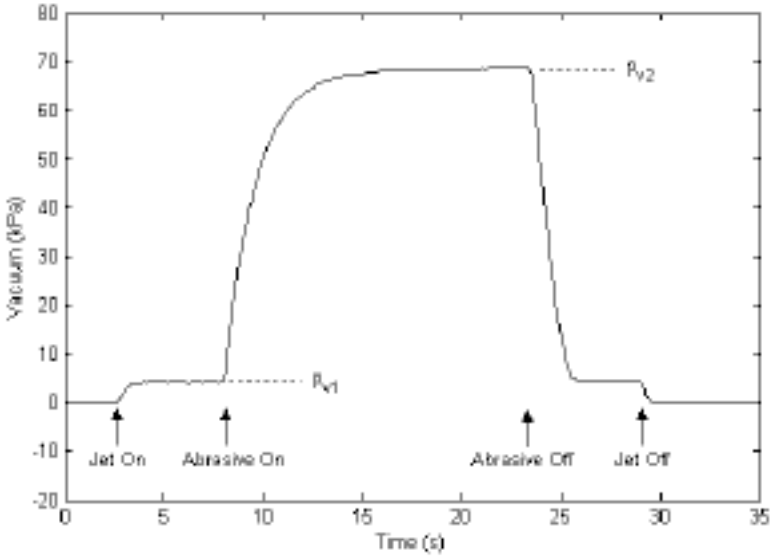

Figure 2: Typical vacuum changes during jet/abrasive switching

2. EXPERIMENTAL SETUP

The basic experimental setup (Figure 3a) consists of an intensifier pump unit with variable pressure delivery from 50 to 379 MPa, a single stationary AWJ cutting head, a single abrasive supply hopper with a variable-aperture metering valve for flow rate control, and a set of transducers for measuring the water pressure and abrasive feed tube vacuum. A USB-based I/O device delivers the transducer signals to a computer, and also allows on/off control of the intensifier pump through the computer software interface. The software samples the continuous transducer signals at 100 ms intervals and stores the data for later analysis. Calibration of the transducer signals for data capture is performed using separate mechanical gauges for the water pressure and vacuum. An analog high pressure gauge is permanently installed in the high pressure plumbing, and a removable analog vacuum gauge can be attached to the vacuum tap fitting in place of the transducer tube. The jet and abrasive on/off valves are controlled by pneumatic actuators, with their respective air supplies switched by separate manual air valves.

The AWJ nozzle is set up with a .254/.762 mm orifice/mixing tube combination, supplied with 80-mesh garnet abrasive at flow rates adjustable from 1.51 to 6.05 g/s. The nominal abrasive mass flow rate for each experimental run is determined from the metering valve aperture setting, based on separately collected calibration data. The abrasive material is transported from the metering valve to the jet nozzle through a 1.5 m length of 6.35 mm ID flexible polyurethane tubing. When the abrasive flow is shut off, the metering valve end of the abrasive feed tube is effectively open to the atmosphere. For measuring the feed tube vacuum, a sealed tap fitting made from a modified brass compression tee is installed on the tube a few centimeters from the mixing chamber inlet. The tap fitting arrangement (Figure 3b) maintains a continuous feed tube interior surface to mimize any disturbance of the air and abrasive flow within the tube.

To allow further investigation of the mechanisms affecting the air inflow rate and the strength of the produced vacuum, the feed tube can also be set up in an abrasive diverter arrangement, as shown in Figure 3c. In this configuration, the metered abrasive flow travels most of the length of the feed tube in the normal way, but is diverted into a sealed reservoir just before reaching the mixing chamber inlet. The vacuum is measured at a point between the chamber inlet and the reservoir. The vacuum increase when the abrasive flow begins thus depends on the restrictive effect of the abrasive particles on an air flow sustained by the water jet alone, without abrasive mixing. Comparing vacuum measurements made this way with those from a fully mixed jet under the same pressure and abrasive flow conditions reveals the effect of abrasive/water mixing on vacuum creation. (For such comparisons, the vacuum measurements made in the diverter configuration must be corrected for the additional exit and entrance effects introduced by the two feed tube attachments to the reservoir lid.) With the volume of the reservoir known (0.00228 m^3), the diverter arrangement can also be used to measure the air transport capacity of the water jet at various pump pressures, as explained in the following section.

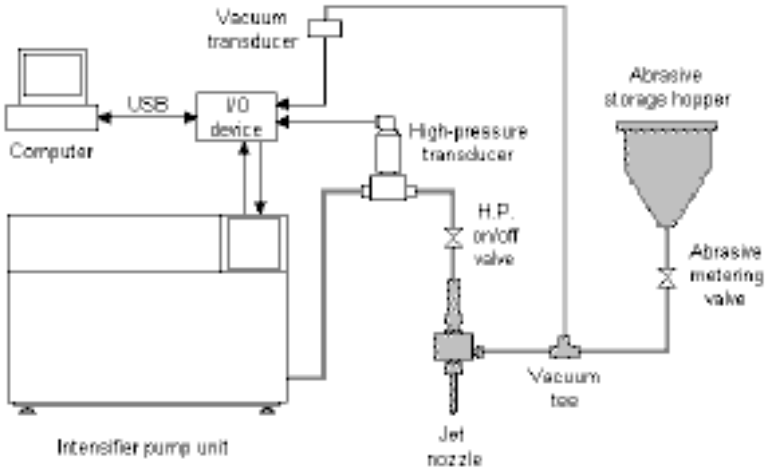

Figure 3a: Experimental setup

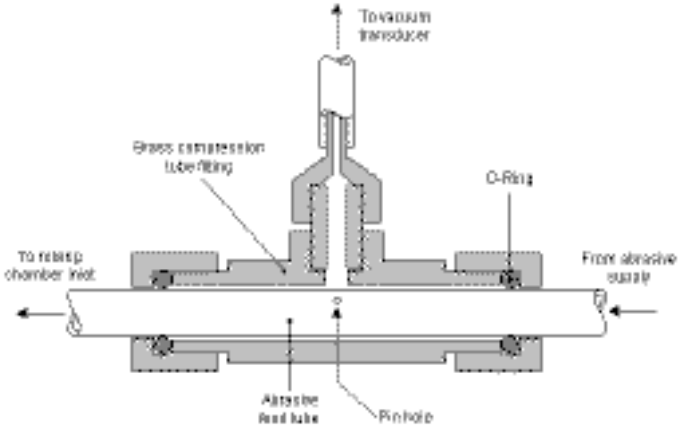

Figure 3b: Vacuum tap fitting

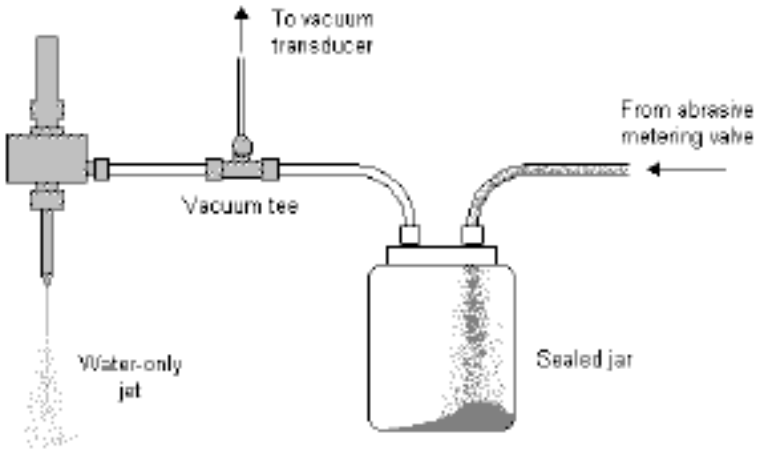

Figure 3c: Abrasive flow diverter setup

3. METHOD

As a starting point for the derivation to follow, we need some sense of whether it is valid to regard the air entrainment rate of the jet to be roughly independent of abrasive/water mixing effects. A related question is whether a simple relationship can be established between the jet pressure (or velocity) and the mass (or volume) flow rate of air through the nozzle under water-only operation. Insight into these issues can provide the basis for certain simplifying assumptions about the air transport rate through the nozzle before and after the start of abrasive flow.

3.1 Air Transport Behavior of the Water-Only Jet

By sampling vacuum (p_{v1}) and pump pressure (p_p) data at frequent intervals as the pressure is slowly raised through its entire adjustment range, a plot of p_{v1} vs. the pump pressure can be obtained, as in Figure 4a. With no abrasive flow and the geometry of the inlet passage fixed, p_{v1} should depend in a predictable way on the air flow rate through the feed tube; thus the p_{v1} vs. p_p relationship should be sufficient to form a basic understanding of the air transport behavior of the jet under water-only operation.

A reasonable first conjecture would be that the air flow rate through the nozzle is proportional to the jet velocity. Neither quantity can be measured directly with the available apparatus, but the assumption can still be tested on the basis of pressure and vacuum measurements alone. The water velocity v_w can be derived from the pump pressure p_p as

$$v_w = \sqrt{2\int_0^{p_p} \frac{1}{\rho_w}\, dp} \tag{1}$$

where the water density ρ_w depends on the pressure p according to

$$\rho_w = \rho_{w0}\left(1 + \frac{p}{\alpha}\right)^{\beta} . \tag{2}$$

Here, α = 300 MPa and β = 0.1368 are experimentally determined constants, and the reference density of water is ρ_{w0} = 1000 kg/m^3. Combining these gives

$$v_w = \sqrt{\frac{2\alpha}{\rho_{w0}(1-\beta)}\left[\left(1 + \frac{p_p}{\alpha}\right)^{1-\beta} - 1\right]} . \tag{3}$$

From familiar friction loss relationships [4], the vacuum level p_{v1} with no abrasive in the air stream can be expected to vary as the square of the air velocity v_{a1} in the feed tube:

$$p_{v1} \quad v_{a1}^{\ 2}. \tag{4}$$

Hence if the air velocity is proportional to the jet velocity, it should appear that

$$\sqrt{p_{v1}} \quad v_w \tag{5}$$

which can be verified by pressure and vacuum measurements only. Applying (eq.3) to the pressure data in Figure 4a and using the square root of p_{v1} on the vertical axis gives the plot shown in Figure 4b. This does imply a roughly linear relationship between v_w and the air velocity within the feed tube, and, equivalenty, between v_w and the volumetric flow rate of air through the nozzle.

Another relatiohship of interest is that between the jet velocity and the air mass flow rate, $\dot{m}_a$. As p_{v1} is relatively small even at high jet pressures, the variation in mixing chamber air density over the water pressure range should be small as well, and $\dot{m}_a$ should stay in approximately fixed proportion to the volumetric air flow rate. One way of estimating the air mass transport rate at a particular jet pressure is to observe the vacuum rise as the jet evacuates a sealed air reservoir of known volume. The abrasive diverter setup shown in Figure 3c is used for this, with the abrasive source detached. The jet is first allowed to run with air flowing in freely from the atmosphere through the reservoir inlet, until a steady air flow is established, indicated by a steady p_{v1} signal. Then, at a time designated $t = 0$, the reservoir air inlet is sealed off, and the vacuum rises at a rate which depends on the rate of air removal from the reservoir. Starting at $t = 0$, the vacuum p_v should depend on the reservoir air density ρ_{aR} according to

$$p_v = p_0 \left[1 - \left(\frac{\rho_{aR}}{\rho_{a0}}\right)^{\gamma}\right], \tag{6}$$

where p_0 and ρ_{a0} are the atmospheric air pressure and density, and γ is the specific heat ratio, with a value of 1.4 assumed for air. The rate of change of the vacuum is then

$$\dot{p}_v = -p_0\gamma \left(\frac{\rho_{aR}}{\rho_{a0}}\right)^{\gamma-1} \left(\frac{1}{\rho_{a0}}\right) \dot{\rho}_{aR} \tag{7}$$

from which the instantaneous rate of change of the reservoir air density at $t = 0$ is

$$\dot{\rho}_{aR}\Big|_{t=0} = -\frac{\dot{p}_v \rho_{a0}}{p_0 \gamma}\left(\frac{\rho_{a0}}{\rho_{aR}}\right)^{\gamma-1}\Bigg|_{t=0}. \tag{8}$$

With a fixed reservoir volume V_R, the associated air mass flow rate is then

$$\dot{m}_a\Big|_{t=0} = \frac{V_R \rho_{a0} \dot{p}_v}{p_0 \gamma}\left(\frac{\rho_{a0}}{\rho_{aR}}\right)^{\gamma-1}\Bigg|_{t=0}. \tag{9}$$

Also, at $t = 0$, the instantaneous vacuum is simply p_{v1} (the steady state vacuum resulting from air flow through the reservoir and tubing), and the reservoir air density is

$$\rho_{aR} = \left(1 - \frac{p_{v1}}{p_0}\right)^{\frac{1}{\gamma}} \rho_{a0} \qquad (\text{at } t = 0) \tag{10}$$

which gives

$$\dot{m}_a\Big|_{t=0} = \frac{V_R \rho_{a0} \dot{p}_v}{p_0 \gamma}\left(1 - \frac{p_{v1}}{p_0}\right)^{\frac{1}{\gamma}-1}\Bigg|_{t=0}. \tag{11}$$

This initial instantaneous air mass flow rate should equal the rate maintained with the air flowing freely under water-only operation (that is, the rate associated with the p_{v1} vacuum level). Curves of p_v vs. time created in this way (Figure 5a) can thus be used to estimate the air mass flow rates by calculating the initial slope for each pressure case. Figure 5b shows the results for the five pressure cases in Figure 5a, which verify the expectation of approximately linear behavior over the practical jet pressure range.

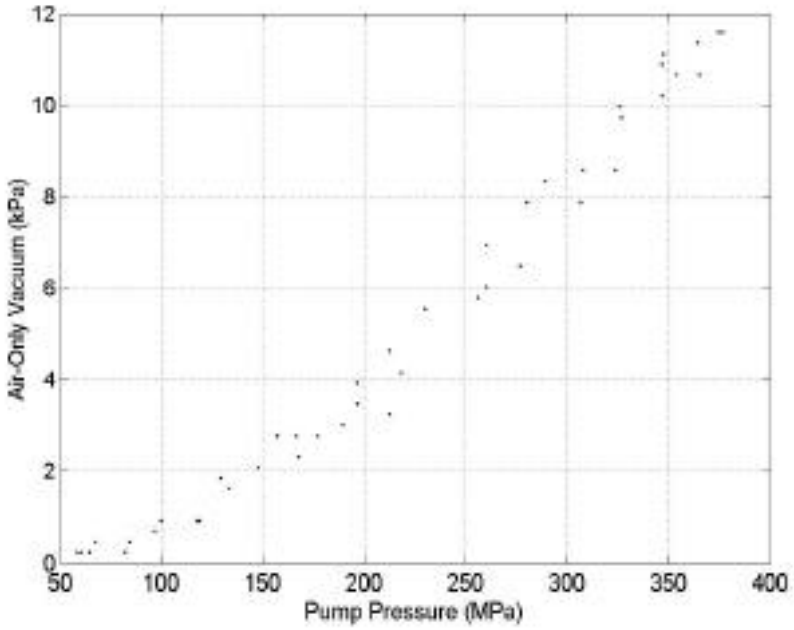

Figure 4a: Vacuum vs. pump pressure with no abrasive flow

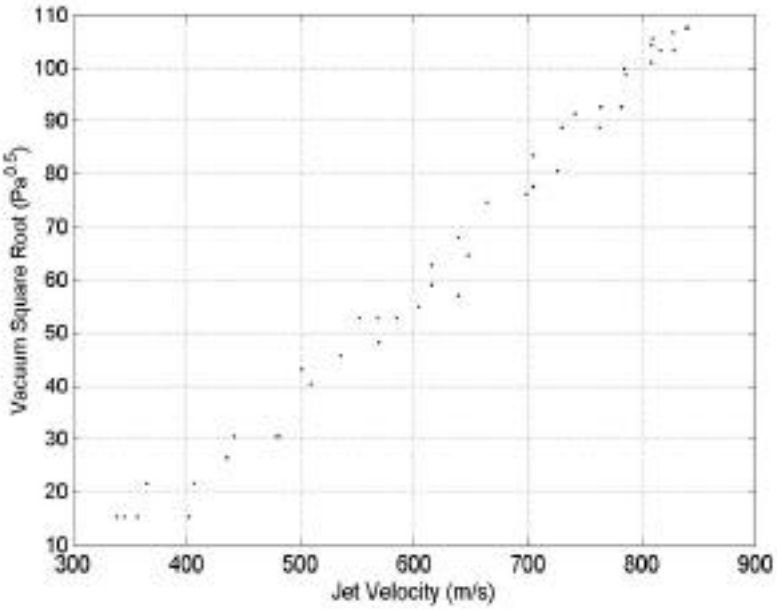

Figure 4b: $p_{v1}^{0.5}$ vs. jet velocity

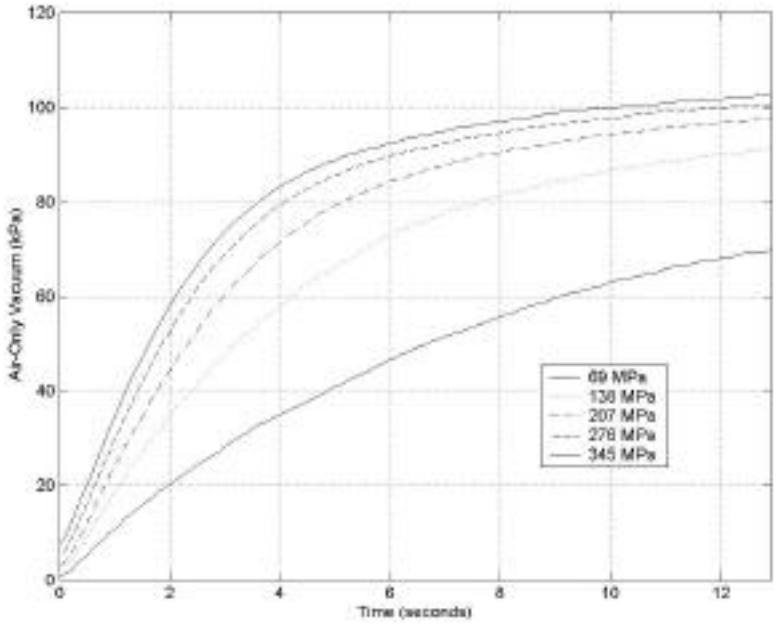

Figure 5a: Evacuation of the reservoir with inlet port sealed

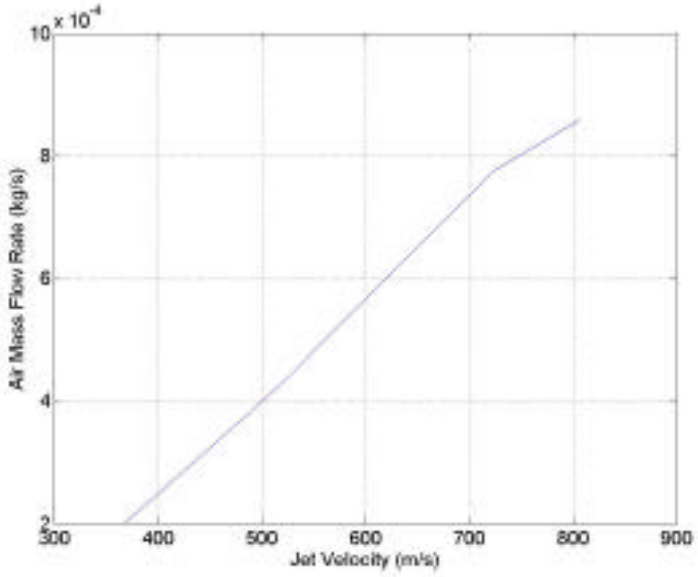

Figure 5b: Air mass flow vs. jet velocity

3.2 Mixing Effects

With some basis established for assumptions about the air transport mechanism under water-only conditions, it remains to be seen how the introduction of abrasive particles to the water stream affects the air flow. The diverter setup of Figure 3c can again be used, this time with the abrasive supply attached so that the air flow restrictions upstream of the reservoir are the same as would be present with the feed tube connected directly to the AWJ nozzle. Vacuum measurements obtained with the abrasive flow diverted are free from the effects of abrasive/water mixing, and can be compared with those of a fully-mixed jet under the same pressure and abrasive flow rate conditions. Figures 6a, b, and c show results obtained at 207, 276 and 345 MPa, with an abrasive flow rate of 3 g/s. The p_{v1} levels are slightly higher in the diverted flow cases, reflecting the slight increase in total air flow restriction with the reservoir connected. However, the p_{v2} level is somewhat reduced by the abrasive diversion, suggesting that the presence of abrasive particles in the water stream does tend to increase the overall air inflow rate. The p_{v2} difference between the mixed and diverted arrangements appears to be smaller at higher pressures, so if a constant air flow assumption is to be applied, the error introduced should be less at higher pressures.

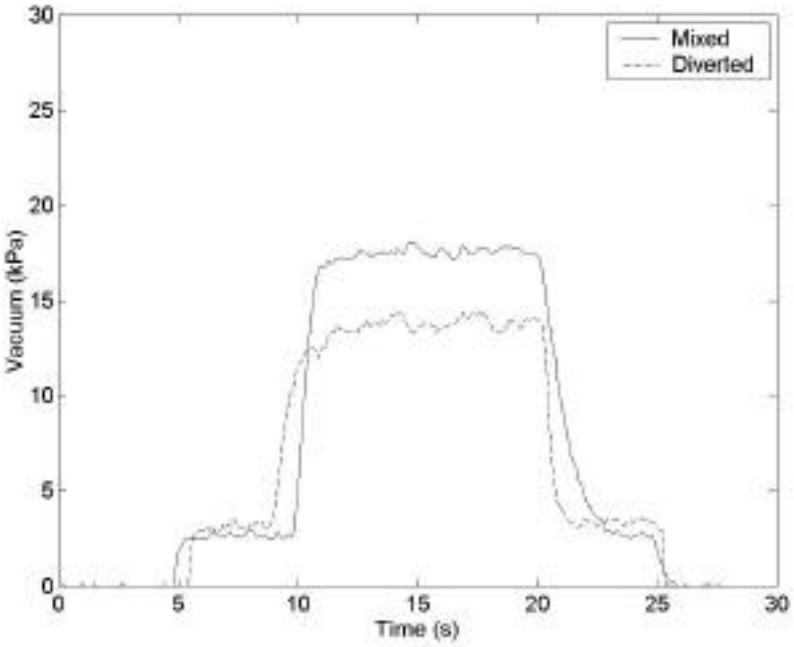

Figure 6a: Mixed and diverted vacuum levels – 207 MPa, 3 g/s

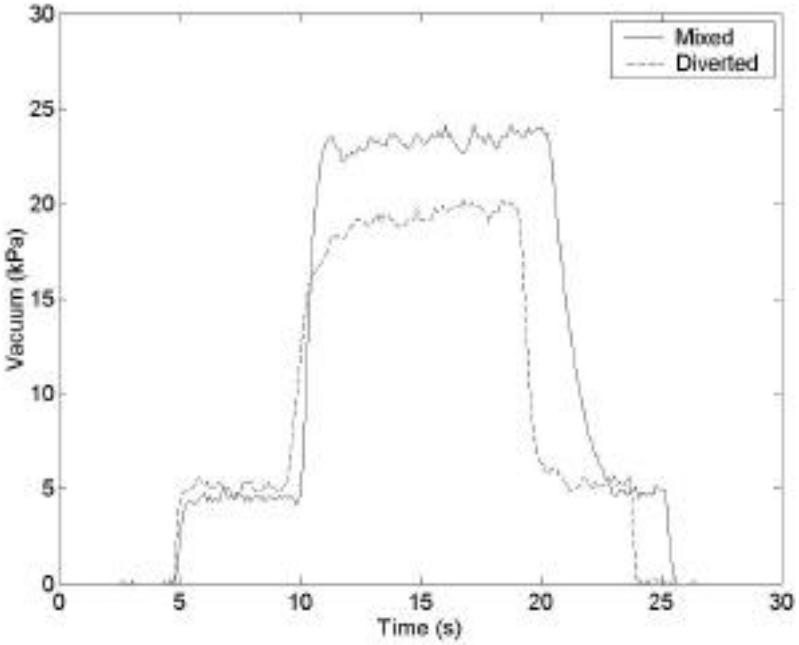

Figure 6b: Mixed and diverted vacuum levels – 276 MPa, 3 g/s

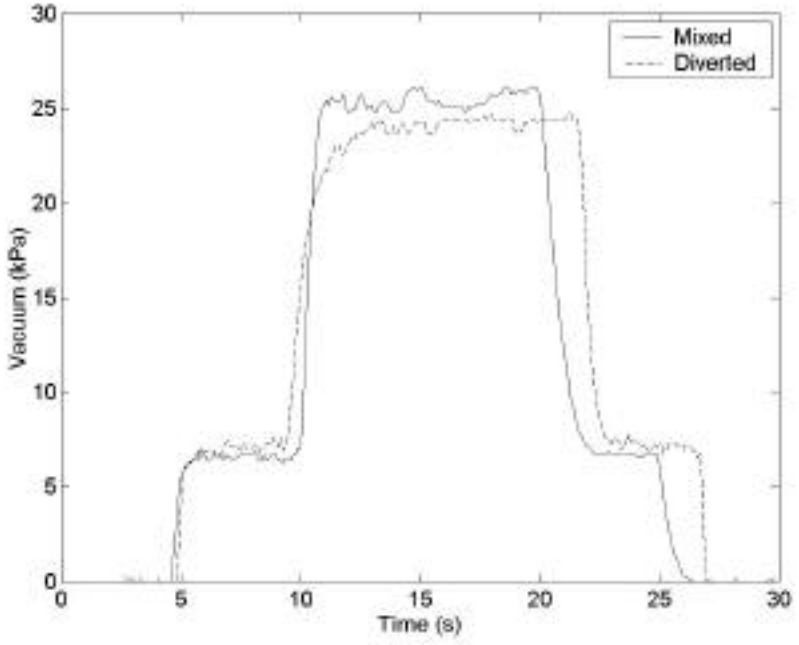

Figure 6c: Mixed and diverted vacuum levels – 345 MPa, 3 g/s

3.3 Effect of Abrasive Mass Flow Rate on Vacuum Rise

Following an analysis of pneumatic transport given in [3], the total pressure change within the mixing chamber (or, more precisely, within the feed tube near its point of attachment to the cutting head) from the initial atmospheric conditions to the final state reached with a fully developed abrasive jet flow is given by

$$\Delta p = \Delta p_L + \Delta p_F + \Delta p_A . \tag{12}$$

Here Δp_L is the pressure loss component associated with the air flow alone (related to the feed tube dimensions and entrance effects), and the other terms are the additional losses due to particle friction and impact (Δp_F) and the acceleration of the particles from rest to their average final velocity within the tube (Δp_A). Determination of precise values for the three pressure loss components is complicated, but certain simplifying assumptions can be made for estimation purposes.

The air flow loss Δp_L under abrasive flow conditions can be taken as approximately equal to that produced by the water jet alone, which can be directly measured by operating the jet without the abrasive. Hence, with vacuum pressure p_{v1} regarded as a positive value as in Figure 2,

$$\Delta p_L = p_{v1} . \tag{13}$$

Assuming a steady, dilute phase air/abrasive flow, the friction and impact component is given by [3]

$$\Delta p_F = \lambda_F \left(\frac{\dot{m}_p}{\dot{m}_a} \right) \left(\frac{L_t}{d_t} \right) \left(\frac{\rho_{a0} v_a^2}{2} \right) \tag{14}$$

where $\dot{m}_p$ and $\dot{m}_a$ are respectively the abrasive and air mass flow rates in the feed tube, L_t and d_t the length and diameter of the tube, ρ_{a0} the initial air density, v_a the air velocity, and λ_F a dimensionless friction factor related to the drag coefficient and settling velocity values of individual abrasive particles.

Lastly, the acceleration component is found from a force and momentum change balance on a differential volume of the air/abrasive mixture in the tube. If the area of the tube internal cross section is A, and the air velocity v_a is assumed constant, the differential pressure drop dp and particle velocity increase dv_p across the volume element are related by

$$A dp = \dot{m}_p dv_p \tag{15}$$

Here, *dp* refers to the differential pressure change due to the acceleration of the particles only. Neglecting the particle volume, the flow area A is related to the air mass flow rate, density, and velocity by

$$A = \dot{m}_a / \rho_a v_a \tag{16}$$

which gives

$$dp = \int_0^{v_p} \rho_{a0} v_a \left(\frac{\dot{m}_p}{\dot{m}_a} \right) dv_p , \tag{17}$$

with ρ_{a0} used for the air density throughout the acceleration region. This leads to

$$\Delta p_A = \rho_{a0} v_a v_p \left(\frac{\dot{m}_p}{\dot{m}_a} \right) \tag{18}$$

where v_p is the final abrasive particle velocity reached when the acceleration is complete. This assumes the particles accelerate from rest and are conveyed horizontally through a straight tube.

Combining Equations (12) – (18), and incorporating p_{v2} as the vacuum measurement under steady abrasive flow (so that $\Delta p = p_{v2}$), gives

$$\dot{m}_p = \frac{\dot{m}_a \left(p_{v2} - p_{v1} \right)}{\rho_{a0} \left(\frac{\lambda_F v_a^2 L_t}{2 d_t} + v_a v_p \right)} . \tag{19}$$

Equation (19) provides a relationship between the abrasive mass flow rate and the associated increase in the mixing chamber vacuum level. In practice, p_{v1} and p_{v2} can be directly measured, while further assumptions are necessary to arrive at reasonable estimates for $\dot{m}_a$, v_a, v_p, and λ_F.

The particle velocity v_p at the mixing chamber inlet is often assumed equal to the air velocity v_a, especially at low abrasive flow rates; Equation (19) then becomes

$$\dot{m}_p = \frac{\dot{m}_a \left(p_{v2} - p_{v1} \right)}{\rho_{a0} v_a^2 \left(\frac{\lambda_F L_t}{2 d_t} + 1 \right)} . \tag{20}$$

The air velocity and mass flow rate can be estimated by assuming adiabatic flow through the mixing chamber and velocity parity between the air and water streams within the mixing tube. The adiabatic law establishes the relationship between the absolute pressure p_{ac} and density ρ_{ac} of the air inside the mixing chamber:

$$\frac{p_{ac}}{p_{a0}} = \left(\frac{\rho_{ac}}{\rho_{a0}}\right)^{\gamma}. \tag{21}$$

The steady state vacuum pressure measurement p_{v1}, recorded after the full air velocity has developed in the feed tube but before the abrasive flow begins, can be used to estimate the initial feed tube air velocity, v_{ain1}. Referring to Equation (13), the air-only pressure loss component in a straight feed tube of length L_t and inside diameter d_t is

$$\Delta p_L = p_{v1} = \frac{\rho_{a0} v_{ain1}^2}{2}\left(\lambda_L \frac{L_t}{d_t} + K\right) \tag{22}$$

where λ_L is the Darcy friction factor and K is the combined entrance/exit loss coefficient [4]. Suitable values for K and λ_L can be determined experimentally for a particular feed tube arrangement. As an approximation, $K \approx 1.5$ for a sharp-edged tube entrance and exit, and the value of λ_L for turbulent flow can be estimated from the Reynold's number as

$$\lambda_L = \frac{0.316}{\mathrm{Re}^{0.25}} \tag{23}$$

where $\mathrm{Re} = \rho_{a0} v_{ain1} d_t / \mu_a$, and μ_a is the absolute viscosity of the air. Combining Equations (22) and (23) yields an estimate of v_{ain1} based on the water-only vacuum measurement. Neglecting the change in air density from the tube entrance to the vacuum measurement point (at distance L_t from the entrance), the associated air mass flow rate is then

$$\dot{m}_{a1} = \frac{\pi}{4} d_t^2 v_{ain1} \rho_{a0}. \tag{24}$$

At steady state, there is no ongoing net accumulation or depletion of air mass inside the mixing chamber, so the air must exit through the mixing tube at the same mass flow rate with which it enters through the inlet port. The assumption of proportionality with the jet velocity, justified by Figures 5a and b, provides a means for estimating this air flow rate. The simplest application of this idea is to assume the velocity of the exiting air to be equal to the water jet velocity v_w, which leads to

$$\dot{m}_{a1} = \rho_{ac1} v_w A_{eff} \tag{25}$$

where ρ_{ac1} is the chamber air density and A_{eff} is the effective area of the air flow through the mixing tube (nominally the cross-section area of the mixing tube bore minus that of the water jet). The water velocity v_w can be computed from the system operating pressure according to Equation (3). Using Equation (21) to compute the air density from the vacuum measurement p_{v1} gives

$$\rho_{ac1} = \rho_{a0}\left(\frac{p_0 - p_{v1}}{p_0}\right)^{\frac{1}{\gamma}}. \tag{26}$$

Equations (24) – (26) combine to give the effective area of the outward air flow:

$$A_{eff} = \frac{\pi v_{ain1} d_t^2}{4 v_w}\left(\frac{p_0}{p_0 - p_{v1}}\right)^{\frac{1}{\gamma}}. \tag{27}$$

The effective air flow area through the mixing tube decreases somewhat when the abrasive flow begins due to the added displacement of the solid particles. This is reflected in the increased air induction capacity of the mixed jet, as suggested by Figures 6a, b, and c. However, the assumption of dilute phase flow in the abrasive/air mixture entering the chamber, plus the high density of the particles relative to water, imply that the abrasive/water volume ratio will be small – about 0.15 or less in most practical situations. Hence for abrasive flows that are small relative to the water flow (i.e. the Figure 6c situation) the area reduction can be neglected and A_{eff} held constant in the approximation. If p_{v2} is the final steady state vacuum level with a fully developed abrasive flow, $p_{v2} > p_{v1}$ in general, and the absolute pressure and air density inside the mixing chamber are less than under water-only conditions. Neglecting the effect of momentum transfer between the water and abrasive particles, the jet velocity can be assumed to remain the same, and the new air mass flow rate can be found from p_{v2} by retaining the exit velocity assumption used in (25):

$$\dot{m}_a = v_w A_{eff} \rho_{ac2} = v_w A_{eff} \rho_{a0}\left(\frac{p_0 - p_{v2}}{p_0}\right)^{\frac{1}{\gamma}}. \tag{28}$$

With (27) and (28), and again neglecting the abrasive particle volume fraction in the air stream, the new air velocity at the feed tube inlet is

$$v_a = \frac{\dot{m}_{a2}}{\rho_{a0}}\frac{4}{\pi d_t^2} = v_{ain1}\left(\frac{p_0 - p_{v2}}{p_0 - p_{v1}}\right)^{\frac{1}{\gamma}}. \tag{29}$$

Equations (28) and (29) establish values for $\dot{m}_a$ and v_a for insertion in (19) or (20). Values for the particle friction factor λ_F have been tabulated for a variety of air and solid particle flow conditions [3].

4. RESULTS AND DISCUSSION

For experimental verification, Equation (20) was used, along with (28) and (29), and $\lambda_F = 0.04$, to compute the abrasive mass flow from four sets of vacuum measurements at each of four pump pressures. The setup used an orifice/mixing tube size combination of 0.254 mm / 0.762 mm, with pressures between 138 and 345 MPa, and independently-measured abrasive flow rates

between 1.51 and 6.04 g/s. Figure 7 shows the raw data tracings, and Figure 8 shows a comparison between the measured and computed values of $\dot{m}_p$. The results are tabulated in Table 1.

The development of this algorithm depends fundamentally on the assumptions of Sections 3.1 and 3.2 – namely, that the air induction rate is always proportional to the jet velocity, and that mixing effects can be neglected at high pressures and moderate abrasive flow rates. The goal of these assumptions is to arrive at a simple relationship between the abrasive mass flow rate and the p_{v1}-to-p_{v2} vacuum rise. More specifically, the derivation seeks to rely only on familiar equations governing turbulent air flow and pneumatic transport of solid particles, and avoids the complexities of jet-particle and jet-air interactions inside the mixing chamber and mixing tube. The results displayed in Figure 8 provide some insight into the strengths and limitations of this simplified approach. The highest pressure case seems to yield the closest overall agreement between the calculated and actual abrasive flow rates. This might be expected from a comparison of Figure 6c with Figures 6a and b, which implies that the error introduced by the neglect of mixing effects is smallest when the ratio of abrasive to water flow is smallest. However, practical cutting situations often involve using the highest feasible abrasive flow rate at a particular pressure for maximum cutting power, and mixing phenomena might have a strong influence on the vacuum measurements obtained, as in Figure 6a. Also, there is a clear trend toward increasing underestimation of the abrasive flow rate as $\dot{m}_p$ increases. This could be another manifestation of the increasing importance of mixing effects at higher abrasive flows, and perhaps of the diminishing validity of the dilute and steady particle flow assumption of Equation (14).

The abrasive mesh size, particle density and shape factor, and other properties of the abrasive material can also be expected to affect the application of the model, particularly in the assignment of a value for λ_F in Equation (14) [3]. No abrasive properties appear explicitly in the final equations yielding $\dot{m}_p$; rather, they are all accounted for by the single parameter $\lambda_{F.}$ Further experiments with different abrasive materials and mesh sizes are necessary to determine whether the customary methods finding λ_F yield good results from Equations (19 and 20) in general.

5. SUMMARY AND CONCLUSIONS

AWJ nozzle can be modeled as a generic vacuum source, tending to produce air flow in the feed tube at a rate which is not strongly dependent on abrasive/water mixing effects within the mixing chamber. The preliminary model developed here for estimation of abrasive mass flow rate is simplified greatly, since the vacuum rise associated with the start of abrasive flow can then be attributed entirely to the restrictive effect of the abrasive particles moving through the feed tube. However, many factors besides the abrasive mass flow rate will influence the vacuum level produced under any nominal set of operating conditions. Orifice and mixing tube wear, particularly, lead to significant variations in air entrainment and vacuum creation over time. Alignment of the orifice and mixing tube are also critical for proper jet function.

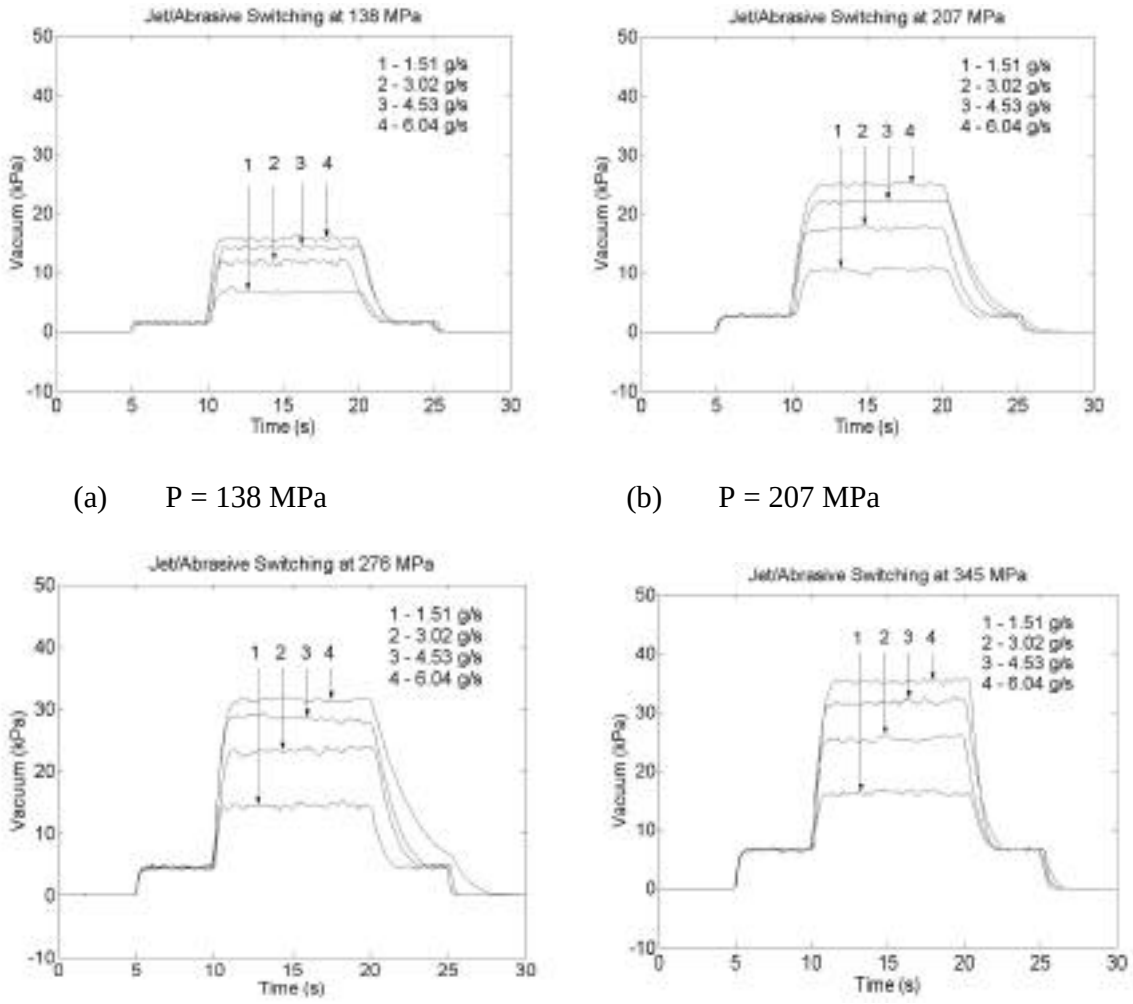

(a) P = 138 MPa (b) P = 207 MPa

(c) P = 276 MPa (d) P = 345 MPa

Figure 7: Effects of jet/abrasive switching on vacuum at different abrasive flow rates

REFERENCES

[1] P. J. Singh, and J. Muñoz, "The Alignability of Jet Cutting Orifice and Nozzle Assemblies," *Proceedings of the 10th International Symposium on Jet Cutting Technology*. Elsevier Applied Science, 1991.

[2] J. Zeng, and J. Muñoz, "Feasibility of Monitoring Abrasive Waterjet Conditions By Means of a Vacuum Sensor," *12th International Conference on Jet Cutting Technology*. London: Mechanical Engineering Publications Limited, 1994.

[3] G.E. Klinzing, et al., *Pneumatic Conveying of Solids*. 2nd Edition. London: Chapman & Hall, 1997.

[4] Frank M. White, *Fluid Mechanics*. 2nd Edition. McGraw-Hill, 1986.

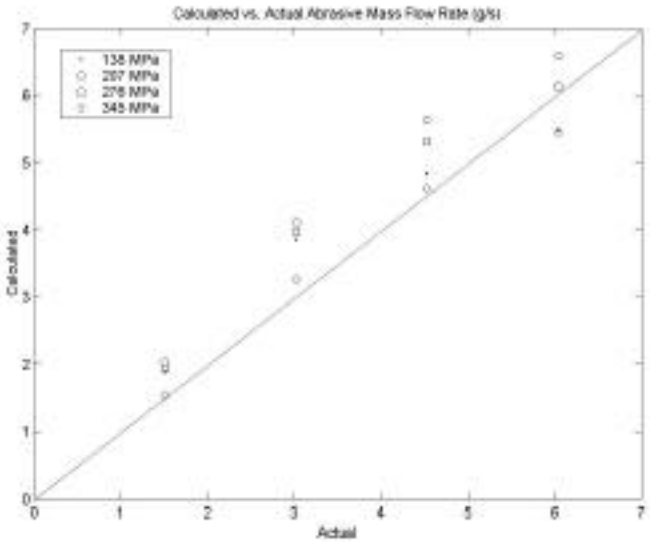

Figure 8: Predicted vs. measured abrasive mass flow rates

Table 1: Vacuum measurements for abrasive flow calculation
(λ_F = 0.04, d_p = 190 μm, d_n/d_m = 0.254/0.762 mm, d_t = 6.35 mm, L_t = 1.5 m)

p_p (MPa)	p_{v1} (Pa)	p_{v2} (Pa)	$\dot{m}_a$ (g/s)	v_a (m/s)	$\dot{m}_p$ (g/s) Measured	$\dot{m}_p$ (g/s) Calculated
138	1452	6698	0.584	15.4	1.51	1.89
138	1452	11771	0.562	14.8	3.02	3.86
138	1452	14153	0.551	14.5	4.53	4.84
138	1452	15675	0.544	14.3	6.04	5.49
207	2649	10426	0.802	21.1	1.51	2.04
207	2649	17470	0.758	19.9	3.02	4.11
207	2649	22160	0.728	19.2	4.53	5.64
207	2649	24909	0.710	18.7	6.04	6.59
276	4589	14451	1.07	28.2	1.51	1.93
276	4589	23346	0.993	26.1	3.02	3.97
276	4589	28488	0.947	24.9	4.53	5.31
276	4589	31443	0.920	24.2	6.04	6.14
345	6610	16249	1.31	34.6	1.51	1.54
345	6610	25402	1.21	31.9	3.02	3.26
345	6610	31683	1.14	30.1	4.53	4.62
345	6610	35217	1.10	29.0	6.04	5.46